Analytical Methods

Cite this: *Anal. Methods*, 2011, **3**, 2604

www.rsc.org/methods

PAPER

Determination of peroxodisulfate ion using composite film containing naphthol green B and multi-walled carbon nanotubes†

Yogeswaran Umasankar,‡ Shih-Hong Wang and Shen-Ming Chen*

Received 14th April 2011, Accepted 24th August 2011
DOI: 10.1039/c1ay05222e

An electrochemically active composite film which contains multi-walled carbon nanotubes (MWCNTs) incorporated with naphthol green B (NGB) was synthesized on glassy carbon, gold and indium tin oxide electrodes by potentiodynamic method. The presence of MWCNTs in the composite (MWCNTs-NGB) film modified electrodes mediates redox reaction of $Fe^{III/II}$ present in NGB, whereas no redox reaction of NGB occurred at the bare electrode. The electrochemical impedance spectroscopy studies revealed that NGB and MWCNTs present in MWCNTs-NGB composite film enhances electron shuttling between the reactant and electrode surface. The surface morphology of the MWCNTs and MWCNTs-NGB were studied using atomic force microscopy, which revealed that NGB incorporated and covered the MWCNTs on the modified electrode. The MWCNTs-NGB composite film exhibits promising enhanced electrocatalysis towards $S_2O_8^{2-}$. The response of $S_2O_8^{2-}$ at MWCNTs and MWCNTs-NGB composite films was measured using both cyclic voltammetry and i–t curve techniques. The linear concentration range of $S_2O_8^{2-}$ determination at MWCNTs-NGB composite film was from 15.9 μM to 7.1 mM. The sensitivity of MWCNTs-NGB composite film towards $S_2O_8^{2-}$ was $-301.9\ \mu A\ mM^{-1}\ cm^{-2}$, and the limit of detection was 6.9 μM. These above values are better than the values obtained at MWCNTs film.

Introduction

Naphthol green B or acid green (NGB) is an important dye with a pseudooctahedral Fe^{III} complex containing 1-nitroso-2-naphthol-6-sulfonate in the deprotonated state as a bidentate ligand. Literature shows that NGB's electrochemical properties were already studied. These reports revealed that in the presence of Fe^{III} the NGB compound undergoes excellent redox reaction, and NGB adsorbs well on the electrode surfaces.[1,2] Both these properties of NGB are required for good redox reactions. Therefore, immobilization of NGB on an electrode is a potential method for developing electrochemical sensor devices. Similar dye compounds such as nitroso and azine dyes have wide use in electrochemistry as redox indicators and mediators.[3] Some of these dyes also have open but ionized structure, and hence the resulting matrix exhibits interesting features like a fast rate of charge transfer, ion transport and good catalytic ability towards molecular reactions.[4]

A wide variety of matrices made of carbon nanotubes (CNTs) were reported in the literature for the determination of bio-organic and inorganic compounds.[5–8] The rolled-up graphene sheets of carbon, *i.e.*, CNTs, exhibit π-conjugative structures with highly hydrophobic surfaces. This property of CNTs allows them to interact with some organic aromatic compounds through π–π electronic and hydrophobic interactions.[9–11] These interactions were used for preparing composite sandwiched films for electrocatalytic studies[12] and in the designing of nano devices with the help of non-covalent adsorption of compounds on the side walls of CNTs.[13] Some attempts were also made to prepare hydrophilic surface CNTs to overcome the dispersion problems in aqueous medium for electrochemical applications.[14] Even though the electrocatalytic activity of CNTs or dye matrices individually showed good results, some properties like mechanical stability and sensitivity for different techniques are found to be poor. However, NGB is an anion and thus it can be incorporated into various matrices as a dopant.[1] Therefore in this work, an attempt has been made for the preparation of a composite film made of CNTs and NGB. Electrodes modified with composite films are widely used in capacitors, batteries, fuel cells, chemical sensors and biosensors.[15–17]

Peroxodisulfate ions containing compounds such as potassium persulfate, ammonium persulfate, *etc.*, are used as food additives, oxidizing agents in organic synthesis such as Elbs persulfate oxidation, and whitening agents with hydrogen peroxide in hair dye. Another application of $S_2O_8^{2-}$ includes the preparation of

Department of Chemical Engineering and Biotechnology, National Taipei University of Technology, No.1, Section 3, Chung-Hsiao East Road, Taipei, 106, Taiwan (ROC). E-mail: smchen78@ms15.hinet.net; Fax: +886 2270 25238; Tel: +886 2270 17147

† Electronic supplementary information (ESI) available. See DOI: 10.1039/c1ay05222e

‡ Present address: Faculty of Engineering, University of Georgia, Athens, GA 30602, USA.

emulsion polymerization initiators. Because of its wide usage in the environment, the detection and determination of $S_2O_8^{2-}$ becomes essential. In the past, various determination methods were developed for the detection of $S_2O_8^{2-}$.[18–20] However, development of more sensitive and reliable methods is necessary; because some methods have limitations, for example unmodified electrodes such as glassy carbon electrodes (GCE) have pronounced fouling effect, poor selectivity, and reproducibility. To overcome these limitations, electrodes were modified using catalysts such as CNT with chitosan,[21] zinc oxide/zinchexacyanoferrate, ruthenium oxide hexacyanoferrate hybrid film,[22] *etc.* The sensitivity of CNT-chitosan was 2.05×10^{-2} μA μM^{-1} with the linear range of 1.6–24 μM $S_2O_8^{2-}$. To further improve the $S_2O_8^{2-}$ determination efficiency, in this work we prepared a composite film (MWCNTs-NGB) made of multi-walled carbon nanotubes (MWCNTs) incorporated with NGB. MWCNTs-NGB composite films' characterization, peak current and electrocatalysis activity have been reported along with its application in the determination of $S_2O_8^{2-}$. The MWCNTs-NGB composite film formation processing involves the modification of electrodes with uniformly well dispersed MWCNTs, and which is then modified with NGB.

Experimental

Materials

NGB, MWCNTs (outer diameter = 7–15 nm, inner diameter = 3–6 nm and length = 0.5–200 μm) and $K_2S_2O_8$ obtained from Aldrich and Sigma-Aldrich were used as received. All other used chemicals were of analytical grade. The aqueous solutions were prepared using twice distilled deionized water. Solutions were deoxygenated by purging with pre-purified nitrogen gas. Phosphate buffer solution (PBS) pH 7.0 was prepared from 0.1 M Na_2HPO_4 and 0.1 M NaH_2PO_4 aqueous solutions, and then pH 4.5 aqueous solution was prepared from 0.1 mM $C_2O_4H_2$.

Apparatus

Cyclic voltammetry (CV) was performed using analytical system models CHI-1205 potentiostat. A conventional three-electrode cell assembly consisting of an Ag/AgCl reference electrode and a Pt wire counter electrode were used for electrochemical measurements. The working electrode was GCE modified either with NGB, MWCNTs or MWCNTs-NGB composite film. In all the experimental results potential is reported *versus* Ag/AgCl reference electrode. The working electrode used for the electrochemical quartz crystal microbalance (EQCM) measurements was an 8 MHz AT-cut quartz crystal coated with gold electrode. The diameter of the quartz crystal is 13.7 mm; the gold electrode diameter is 5 mm. Electrochemical impedance spectroscopy (EIS) measurements were performed using IM6ex ZAHNER (Kroanch, Germany). The morphological characterizations of various films were examined by means of atomic force microscopy (AFM) (Being Nano-Instruments CSPM4000). The amperometric (i–t curve) measurements were performed using CHI-750 potentiostat with analytical rotator AFMSRX (PINE instruments, USA). All the measurements were carried out at 25 °C ± 2.

Preparation of MWCNTs-NGB composite film modified electrodes

The important challenge in the preparation of MWCNTs solution for electrode modification was the difficulty in dispersing it in to a homogeneous solution. Generally, the dispersion of CNTs were carried out by physical (milling) and chemical methods (covalent and noncovalent functionalization). Briefly, by following previously reported methods[23,24] 50 mg of MWCNTs were heated at 350 °C for 2 h to remove the amorphous carbon impurities, and then cooled to room temperature. These heat treated MWCNTs were ultrasonicated for 4 h in 20 ml conc. HCl to remove other impurities, and washed several times with water and then dried at 100 °C in an air oven. These purified and dried MWCNTs were acid treated using sulfuric acid and nitric acid (3 : 1) by 6 h ultrasonication at room temperature, and then washed several times with water until the pH of the supernatant was neutral. These acid treated MWCNTs have been dried overnight at 60 °C. Finally the uniform dispersion of MWCNTs was obtained by 6 h ultra sonication of acid treated MWCNTs in water.

Before starting each experiment, GCEs were polished by BAS polishing kit with 0.05 μm alumina slurry, then rinsed and then ultrasonicated in double distilled deionized water. The GCEs studied were uniformly coated with 50 μg cm^{-2} of MWCNTs and dried at room temperature. The exact quantity of homogeneously dispersed MWCNTs drop coated over GCEs by using micro-syringe. The electrochemical deposition of NGB on MWCNTs modified GCE was performed from 1 mM NGB in 0.1 mM $C_2O_4H_2$ (pH 4.5) aqueous solution by consecutive cyclic voltammograms over a suitable potential region of 0.5 to −0.3 V with scan rate of 50 mVs^{-1}. Then the MWCNTs-NGB modified GCE was carefully washed with double distilled deionized water. In real sample analysis, concentration of the sample was calculated using standard addition plot, where known and unknown $S_2O_8^{2-}$ current values were used for calculation. For obtaining electroanalytical results, i–t curve results of both real sample and a prepared sample containing same concentrations of $S_2O_8^{2-}$ were used.

Results and discussions

Electrodeposition of NGB at various electrodes and their characterizations

The electrochemical deposition of NGB (1 mM) on MWCNTs modified GCE present in $C_2O_4H_2$ aqueous solution was performed by consecutive cyclic voltammograms for the preparation of MWCNTs-NGB composite film. The suitable potential range for NGB deposition is 0.5 to −0.3 V. On subsequent cycles the cyclic voltammograms showed redox peak current corresponding to NGB increased at MWCNTs modified GCE (Fig. 1 inset). This result indicates that during the cycle, deposition of NGB took place on MWCNTs modified GCE. The possible adsorption site of NGB at MWCNT is given in Scheme 1. The docking of NGB on acid treated MWCNTs has been carried out using Lamarckian genetic algorithm in ArgusLab.[25–28] The simulation conditions such as population size (50), maximum generations (3000), crossover rate (0.8), mutation rate (0.2), elitism (5), local search rate (0.06) and local search maximum

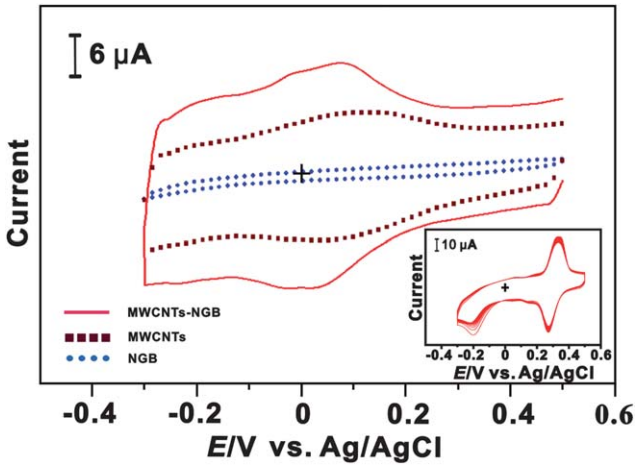

Fig. 1 Cyclic voltammograms of NGB, MWCNTs and MWCNTs-NGB film modified GCEs in PBS, potential between 0.5 and −0.3 V with scan rate of 50 mV s^{-1}. Inset is the repetitive cyclic voltammograms (20 cycles) of NGB at MWCNTs modified GCE using 1 mM NGB in 0.1 mM pH 4.5 $C_2O_4H_2$ aqueous solution with 50 mV s^{-1} scan rate.

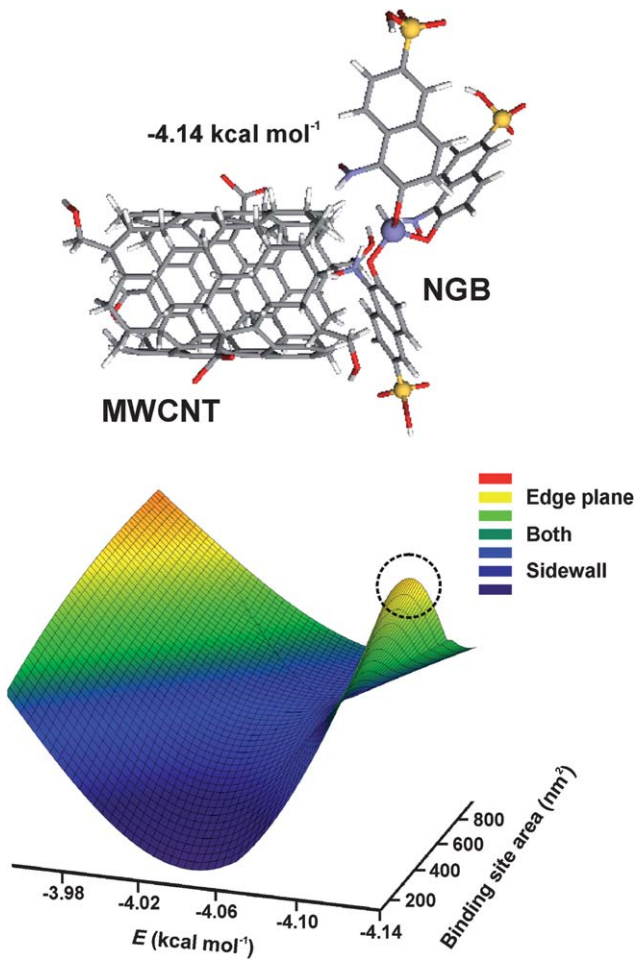

Scheme 1 Possible adsorption site of NGB at MWCNT given by Lamarckian genetic algorithm. The plot in the scheme shows the change in free energy with respect to binding site area and binding site (sidewall, edge plane or both). The circle in the plot indicates the lowest free energy and possible binding site.

steps (100) were kept constant and the area around the binding site was varied to obtain the lowest free energy possible. The plot of free energy *vs.* binding site area and binding site in Scheme 1 shows that the lowest free energy was obtained if the binding site area around MWCNT is 375 nm^2. The minimum free energy obtained was −4.14 kcal mol^{-1}. The same plot shows that free energy reduces while the binding site area increases up to 375 nm^2, however the increase in binding site area after 375 nm^2 increases the free energy at the rate of 0.3 cal mol^{-1} nm^{-2}. The vertical axis with various colours in the Scheme 1 plot shows binding sites such as sidewall, edge plane or both. These data were collected by running numerous simulation experiments at the same mentioned conditions, where each run had its own results. From the collected data, the most possible binding site and its free energy are indicted by the circle in the plot, where the free energy is −4.14 kcal mol^{-1} and the binding site is edge plane of MWCNT.

The above prepared MWCNTs-NGB composite film along with NGB and MWCNTs films were characterized using various electrochemical techniques in PBS. Before electrochemical characterizations, the prepared films were washed carefully in deionized water to remove the loosely attached NGB and $C_2O_4H_2$ present on the modified GCEs. Fig. 1 shows MWCNTs-NGB composite modified GCE's reversible redox couple, MWCNTs modified GCE (absence of NGB) and NGB film modified GCE in PBS. The corresponding cyclic voltammograms were measured at a 50 mVs^{-1} scan rate in the potential range of 0.5 and −0.3 V. Among these three cyclic voltammograms the $E^{\circ\prime}$ of redox couple of MWCNTs-NGB is at 54 mV, where the redox couple represents the redox reaction of $Fe^{III/II}$ present in NGB.[1,2] Similarly the redox reaction of MWCNTs is represented by the redox couple at $E^{\circ\prime}$ = 70.5 mV, whereas there is no redox reaction of NGB present on bare GCE.

The Epa, Epc and Ipc values of MWCNTs and MWCNTs-NGB composite film modified GCEs are given in Table 1. From the Ipc values, surface coverage concentration (Γ) of Fe^{III} species present in MWCNTs-NGB composite film modified electrode is given in Table 1. The Γ of NGB has been calculated using the equation $\Gamma = Q/nFA$, where Q is the charge involved in the reaction, n the number of electrons transferred, F the Faraday constant, and A is the geometric area of the electrode. The Q values were calculated using CHI software. The geometric area of GCE is 0.08 cm^2, and the number of electrons involved in NGB redox reaction is one. The effective area of electrodes was also calculated using Randles-Sevcik equation, and the values are 0.032 cm^2 for bare GCE, 0.033 cm^2 for NGB, 0.036 cm^2 for MWCNTs, and 0.043 cm^2 for MWCNTs-NGB composite film modified GCE. These above results show that the presence of MWCNTs in MWCNTs-NGB composite film enhances the effective area of the electrode by 2 μm^2 μg^{-1}.

EQCM studies of MWCNTs-NGB composite film

The EQCM experiments were carried out by modifying the gold electrode of electrochemical quartz crystal by uniformly coating MWCNTs and then drying at 40 °C. The increase in voltammetric peak current of NGB redox couples and the frequency decrease (or mass increase) are found to be consistent with the growth of NGB film on MWCNTs modified gold electrode (figures not shown). These results too show that the obvious

Table 1 Epa, Epc, Ipc values of redox reactions of MWCNTs and NGB, and surface coverage concentration (Γ) of NGB at MWCNTs modified GCE

Modified Electrodes					
Films	Species	Epa (mV)	Epc (mV)	Ipc (μA)	Γ (nmol cm^{-2})
MWCNTs	—	111	30	2.183	—
MWCNTs-NGB	Fe^{III}	78	30	6.353	1.57

deposition potential has started between 0.5 to −0.3 V. From the frequency change, change in mass of the MWCNTs-NGB composite film at the quartz crystal was calculated by Sauerbrey eqn (1), however 1 Hz frequency change is equivalent to 1.4 ng cm^{-2} of mass change.[29,30] The mass change during NGB incorporation on MWCNTs modified gold electrode for 30 cycles was 30 ng cm^{-2}. The mass change was verified from the voltammetric peak charge of Fe^{III}, where Γ of Fe^{III} in MWCNTs-NGB modified gold electrode for the 30th cycle was 14.8 pmol cm^{-2}. From the Γ value and NGB's molecular weight, the mass of NGB deposited on MWCNTs modified gold electrode for 30 cycles was calculated and it was 13 ng cm^{-2}. This mass change value obtained from the Γ result is less than the mass change value obtained from frequency change. It was because of the formation of byproducts on the electrode surface during NGB deposition. These byproducts do not involve in any electrochemical reaction, so the total mass deposited was high when calculated through Γ results.

$$\text{Mass change } (\Delta m) = -{}^{1}/_{2}\ (f_0{}^{-2})(\Delta f)A(K\rho)^{1}/_{2} \quad (1)$$

Where, f_0 is the oscillation frequency of the crystal; Δf is the frequency change; A, the area of gold disk; K, the shear modulus of the crystal; ρ, the density of the crystal. The scan cycles *vs.* current and frequency change plots of NGB deposition at MWCNTs modified gold electrode are given in the supplementary material.† In these plots, the gross change in peak current of Fe^{III} and the frequency shift over the course of the experiment are found to be consistent. These EQCM results show that the deposition of NGB took place on MWCNTs film.

AFM studies of MWCNTs and MWCNTs-NGB composite films

The MWCNTs and MWCNTs-NGB composite film modified electrodes were prepared on indium tin oxide electrodes with similar conditions as mentioned in the experimental section. Then the bare electrode, MWCNTs and MWCNTs-NGB composite film modified electrodes were characterized using AFM technique. The structures in Fig. 2(a) are the uniformly formed MWCNTs film on the electrode surface from a well dispersed MWCNTs solution. The MWCNTs-NGB composite film in Fig. 2(b) shows a thick layer of NGB deposited over MWCNTs modified electrode. Further in Fig. 2(b), because of the deposition of this thick layer of NGB, the uniform network of MWCNTs is not visible as in Fig. 2(a). Comparison of these AFM results in Fig. 2(a), (b) and (a′) reveal significant morphological difference between all three electrodes, where the uneven structure[31,32] in Fig. 2(a′) is the bare electrode. The thickness of both MWCNTs and MWCNTs-NGB obtained using AFM results were ≈ 290 and 579 nm respectively. These AFM results reveal the coexistence of MWCNTs and NGB as a composite film.

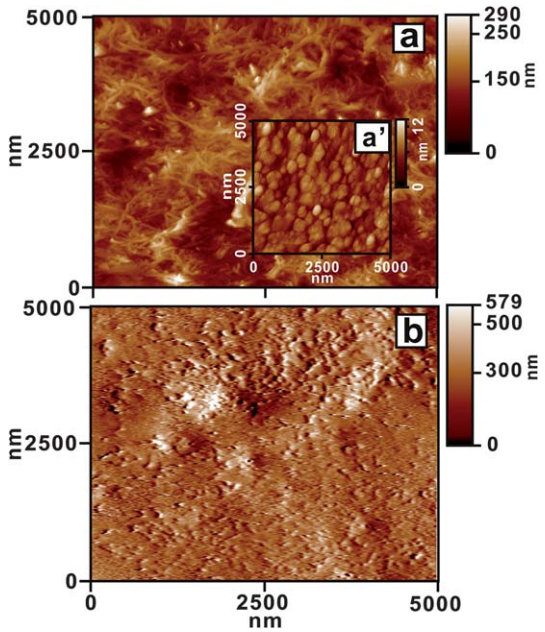

Fig. 2 AFM images of (a) MWCNTs film, (b) MWCNTs-NGB film and (a′) bare electrode.

EIS studies of MWCNTs and MWCNTs-NGB composite films

Fig. 3 shows the impedance spectra represented as Nyquist plots (Z_{im} *vs.* Z_{re}) for bare GCE, MWCNTs and MWCNTs-NGB composite film modified GCEs in 5 mM $Fe(CN)_6{}^{3-/4-}$. Inset in Fig. 3 represents the Randles equivalent circuit model used for fitting the experimental data, where R_s is electrolyte resistance, R_{et} charge transfer resistance, C_{dl} double layer capacitance and Z_w Warburg impedance. The semicircle appeared in Nyquist plot indicates the parallel combination of charge transfer resistance and double layer capacitance resulting from electrode impedance.[33] All the above said films exhibit semicircles with various diameters in the frequency range 0.1 Hz to 1 MHz. In order to find the electron transfer efficiency of the electrodes, R_{et} values were obtained for each modified and unmodified electrode by

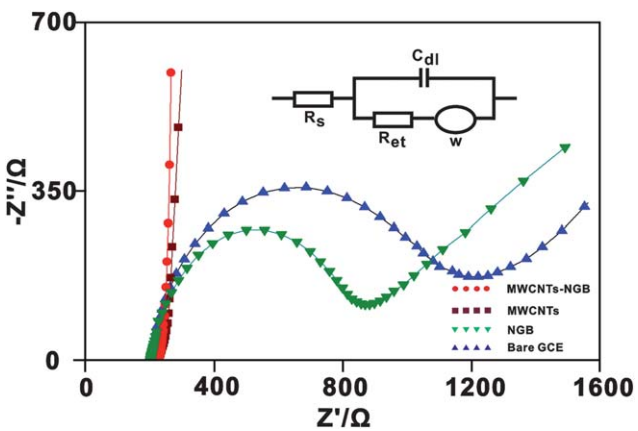

Fig. 3 EIS of bare GCE, NGB, MWCNTs and MWCNTs-NGB modified GCEs in 5 mM $Fe(CN)_6{}^{3-}/Fe(CN)_6{}^{4-}$ in PBS. Amplitude: 5 mV, frequency: 0.1 Hz to 1 MHz. Inset shows the Randles circuit for the above mentioned electrodes.

fitting these above Nyquist plot results with Randles equivalent circuit model. The obtained R_{et} values of bare GCE, NGB, MWCNTs and MWCNTs-NGB composite films are 875.2 kΩ, 644.4 kΩ, 71.52 Ω and 32.8 Ω respectively. These above values show that the presence of NGB decreases the charge transfer resistance of bare GCE and MWCNTs modified GCE. Similarly, the presence of MWCNTs on the electrode also decreases charge transfer resistance. Further, MWCNTs-NGB composite film shows a lower charge transfer resistance than other modified and unmodified electrodes. These results prove that both NGB and MWCNTs present in MWCNTs-NGB composite film enhance electron shuttling between reactant and the electrode surface.

Electrochemical and stability studies of MWCNTs-NGB composite film

The effect of pH on MWCNTs-NGB composite film was studied. Fig. 4 shows the cyclic voltammograms of MWCNTs-NGB composite film modified GCE obtained in various pH aqueous buffer solutions without the presence of NGB in the solution. In these above experiments the MWCNTs-NGB composite film preparation was carried out in $C_2O_4H_2$ aqueous solution as mentioned in the experimental section, and then washed with deionized water before transferring it in to various pH solutions. The results show that the redox reaction of $Fe^{III/II}$ present in NGB was stable in the pH range between 1 and 13, but in higher pH the redox peak current is not as high as in lower pH. Similarly, the $Fe^{III/II}$ redox peaks' Epa and Epc depends on the pH value of the buffer solution. The response from the plot of $Fe^{III/II}$ formal potential *vs.* pH shows the slope of −50.9 mV pH^{-1}, which is close to that given by the Nernstian equation for an equal number of electron and proton transfers.

The stability of NGB on MWCNTs modified GCE in PBS was studied, and the percentage of degradation of MWCNTs-NGB was calculated using an equation given in the literature.[34] The experiment was conducted with the successive 210 min cycling (scan rate 50 mV s^{-1}) applied over a potential range of 0.4 to −0.2 V on MWCNTs-NGB in PBS (figure not shown). The cyclic voltammograms were recorded at the interval of 30 min each, from which the values of Ipc were noted and plotted against time (see supplementary material†). From the results it is clear that after 120 min the response of MWCNTs-NGB becomes constant with time and cycling, indicating it is a stable film. The amount of degradation after 210 min cycling for MWCNTs-NGB was only 9.2%. The above pH and stability results show that the MWCNTs-NGB composite film can be used for electrocatalysis experiments in neutral pH.

Electrocatalysis of $S_2O_8^{2-}$ by MWCNTs-NGB composite film

The NGB, MWCNTs and MWCNTs-NGB composite films were synthesized on GCEs at similar conditions as given in the experimental section. Then these three film modified GCEs were washed carefully in deionized water and separately transferred to PBS for the electrocatalysis of $S_2O_8^{2-}$. All the cyclic voltammograms were recorded at the constant time interval of 2 min with N_2 purging before the start of each experiment. Fig. 5 shows the electrocatalysis reduction of $S_2O_8^{2-}$ (5 mM) at various film modified and unmodified GCEs with scan rate of 50 mV s^{-1}. The various film modified GCEs studied were NGB, MWCNTs and MWCNTs-NGB composite films, where the MWCNTs-NGB composite film is shown with the highest concentration (5 mM) and in the absence of $S_2O_8^{2-}$. The cyclic voltammogram for MWCNTs-NGB composite film exhibits reversible redox couple in the absence of $S_2O_8^{2-}$, and upon addition of $S_2O_8^{2-}$ new growth in the reduction peaks of $S_2O_8^{2-}$ appears at Epc = −36 and −207 mV. Similarly for MWCNT film, the peak current of $S_2O_8^{2-}$ appears at Epc = −88 mV. In these above electrocatalysis experiments, an increase in concentration (0.2 to 6 mM) of $S_2O_8^{2-}$ simultaneously produced a linear increase in reduction

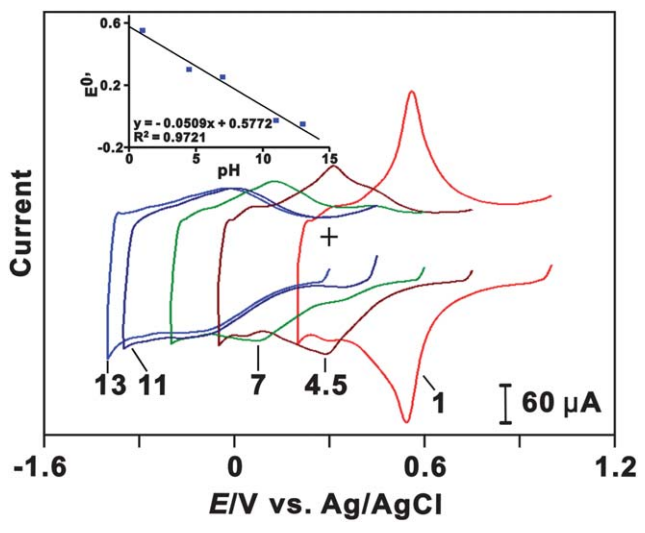

Fig. 4 Cyclic voltammograms of MWCNTs-NGB composite film modified GCE in various pH solutions (scan rate 50 mVs^{-1}). The inset shows the formal potential *vs.* pH from 1 to 13 (slope = −50.9 mV pH^{-1}), where the slope is almost nearer to Nernstian equation for equal number of electron and proton transfers.

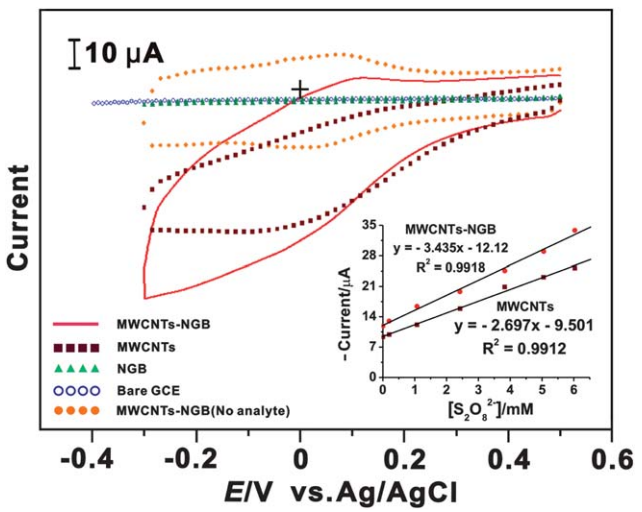

Fig. 5 Cyclic voltammograms of $S_2O_8^{2-}$ (5 mM) at bare GCE, NGB, MWCNTs and MWCNTs-NGB composite film modified GCEs in PBS at 50 mV s^{-1}; where MWCNTs-NGB composite film is shown in both the presence and absence of 5 mM $S_2O_8^{2-}$. The inset is the plot of peak current (Ipc) *vs.* concentration of $S_2O_8^{2-}$ at MWCNTs and MWCNTs-NGB films respectively.

peak currents of $S_2O_8^{2-}$ at both MWCNTs and MWCNTs-NGB films with good film stability. However, there is no reduction peak of $S_2O_8^{2-}$ in the unmodified and NGB film modified GCEs even at 5 mM $S_2O_8^{2-}$.

It is obvious that the MWCNTs-NGB composite film shows higher electrocatalytic activity for $S_2O_8^{2-}$ when comparing MWCNT film. In detail, the enhanced electrocatalytic activity of MWCNTs-NGB composite film can be explained in terms of both lower overpotential and higher peak current of $S_2O_8^{2-}$ than at MWCNT film. These results can be observed from the Epc and Ipc values given in Table 2. Where, the increase in peak current and decrease in overpotential, are considered as the electrocatalytic activity.[35,36] This electrocatalytic activity in MWCNTs-NGB composite film is because of the presence of both MWCNTs and NGB. From the slopes of linear calibration curves (Fig. 5 inset) the sensitivity of MWCNTs (at Epc = −88 mV) and MWCNTs-NGB (at Epc = −36 mV) composite film modified GCEs towards $S_2O_8^{2-}$ and their correlation co-efficients were calculated and are given in Table 2. It is obvious that the sensitivity of MWCNTs-NGB composite film is higher for $S_2O_8^{2-}$ when comparing MWCNT film. From the same results, $S_2O_8^{2-}$'s limit of detection (LOD) at MWCNTs and MWCNTs-NGB composite films at the signal to noise ratio of 3 were calculated and given in the same table. These results show MWCNTs-NGB film possesses lower LOD than MWCNTs film modified GCE. The overall view of these results reveals that MWCNTs-NGB composite film is efficient for $S_2O_8^{2-}$ analysis.

Amperometric studies of $S_2O_8^{2-}$ by MWCNTs and MWCNTs-NGB composite films

Fig. 6 is the amperometric response of MWCNTs and MWCNTs-NGB composite films in i–t curve experiment with successive addition of $S_2O_8^{2-}$ in the concentration range from 15.9 μM to 7.1 mM at the potential of −0.3 V and rotation rate of 1200 RPM. In these results, the amperometric response reaches in about 5 s upon the addition of $S_2O_8^{2-}$ and the response is proportional to its concentration for both modified GCEs. In the above i–t curve experiments an increase in concentration (15.9 μM to 7.1 mM) of $S_2O_8^{2-}$ simultaneously produces a linear increase in reduction current of $S_2O_8^{2-}$ at MWCNTs and MWCNTs-NGB composite films. From the slopes of linear calibration curves (Fig. 6 inset) the sensitivity of MWCNTs and MWCNTs-NGB composite film modified GCEs towards $S_2O_8^{2-}$ and their correlation co-efficient were calculated and are given in Table 2. From the same results, the LOD for $S_2O_8^{2-}$ at MWCNTs and MWCNTs-NGB at the signal to noise ratio of 3 were calculated and given in the same table. These results also show that MWCNTs-NGB composite film was better than the

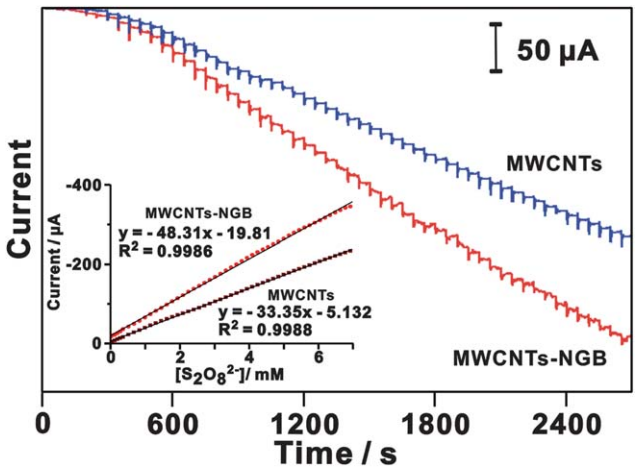

Fig. 6 i–t curve results of MWCNT film and MWCNTs-NGB composite film in PBS (at 1200 rpm and potential = −0.3 V) in the presence of $S_2O_8^{2-}$ at 0, 15.9 μM∼7.1 mM. The inset shows the plot of current *vs.* different concentrations of $S_2O_8^{2-}$ obtained using i–t curve at MWCNT film and MWCNTs-NGB composite film.

MWCNT film. Comparison of previously reported film modified electrodes with MWCNTs-NGB composite film shows MWCNTs-NGB film have lower potential, better sensitivity and LOD values for the $S_2O_8^{2-}$ reduction.[37–39] For example, poly (luminol)/phosphomolybdate films have the reduction peak potential of −120 mV,[37] and copper(II)-nickel(II)hexacyanoferrate film has −400 mV.[38] These potentials are higher than the reduction potential obtained by MWCNTs-NGB film. The heteropolytungstate/CNTs has the sensitivity of 2.05×10^{-2} μA μM^{-1},[21] which is lower than the value obtained for MWCNTs-NGB film. These results show that MWCNTs-NGB composite film can be efficiently used for $S_2O_8^{2-}$ determination.

Real sample (hair bleaching agent) analysis

The performance of MWCNTs-NGB composite film modified GCE was tested by applying it to the determination of $S_2O_8^{2-}$ present in hair bleaching agents. The technique used for the determination was i–t curve, and the experimental conditions

Table 3 Electroanalytical values obtained from the hair bleaching agent's $S_2O_8^{2-}$ determination using i–t curve in PBS by MWCNTs-NGB composite film modified GCE

Added (μM)	Found (μM)	Recovery (%)	RSD (%)
50	50.3	100.7	1.2
200	207.9	103.8	
350	356.8	101.9	

Table 2 Electroanalytical results for $S_2O_8^{2-}$ at various modified GCEs using various techniques in PBS

Technique	Film type	Epc (mV)	Ipc (μA)[a]	Linear range (mM)	Sensitivity (μA mM^{-1} cm^{-2})[b]	LOD (μM)
CV	MWCNTs	−88	23	0.2∼6.0	−33.7[0.9912]	120
	MWCNTs-NGB	−36 and −207	29 and 40	0.2∼6.0	−42.9[0.9918]	97.6
i–t curve	MWCNTs	−300	—	0.0159∼7.1	−208.4[0.9988]	10.1
	MWCNTs-NGB	−300	—	0.0159∼7.1	−301.9[0.9986]	6.9

[a] Concentration of $S_2O_8^{2-}$ = 5 mM. [b] The correlation coefficients are given in parentheses.

were similar to that of amperometric studies given in the previous section. The hair bleaching agent was obtained from Yolanda Co. Ltd., China/Luxuriant Co. Ltd., Canada. The bleaching agent's labeled composition was 25% ammonium persulfate, 25% potassium persulfate and 11% sodium metasilicate. Before the analysis by composite film, the exact $S_2O_8^{2-}$ concentration present in the real sample was measured using standard addition method. The concentrations added in the experiment, found and relative standard deviation (RSD) obtained from the experiments are given in Table 3. From the results given in Table 3 the recovery of $S_2O_8^{2-}$ is $\approx$102%. These above result show that MWCNTs-NGB composite film is efficient for peroxodisulfate ion determination.

Conclusions

Composite material containing MWCNTs and NGB at glassy carbon, gold and ITO electrodes has been reported. The developed MWCNTs-NGB composite film for electrocatalysis combines the advantages of ease of fabrication, high reproducibility and long-term stability. The AFM results have shown the differences between MWCNTs and MWCNTs-NGB composite film morphology. Further, it has been found that MWCNTs-NGB composite film has excellent functional properties along with good electrocatalysis activity on potassium persulfate. The experimental methods of CV and i–t curve with MWCNTs-NGB composite film presented in this article provide an opportunity for qualitative and quantitative characterization of $S_2O_8^{2-}$ sensor.

Acknowledgements

This work was supported by the National Science Council and the Ministry of Education of Taiwan (Republic of China).

References

1 A. Mohadesi and M. A. Taher, *Sens. Actuators, B*, 2007, **123**, 733–739.
2 Q. Zhao, R. Yuan, C. L. Mo, Y. Q. Chai and X. Zhong, *Chinese Chem. Lett.*, 2004, **15**, 208–211.
3 A. A. Karyakin, E. E. Karyakina and H. L. Schmidt, *Electroanalysis*, 1999, **11**, 149–155.
4 Q. Wan, X. Wang, X. Wang and N. Yang, *Polymer*, 2006, **47**, 7684–7692.
5 U. Yogeswaran and S. M. Chen, *Electrochim. Acta*, 2007, **52**, 5985–5996.
6 G. Wu, Y. S. Chen and B. Q. Xu, *Electrochem. Commun.*, 2005, **7**, 1237–1243.
7 J. Wang and M. Musameh, *Anal. Chim. Acta*, 2004, **511**, 33–36.
8 J. Wang, M. Li, Z. Shi, N. Li and Z. Gu, *Electrochim. Acta*, 2001, **47**, 651–657.
9 Q. Li, J. Zhang, H. Yan, M. He and Z. Liu, *Carbon*, 2004, **42**, 287–291.
10 J. Zhang, J. K. Lee, Y. Wu and R. W. Murray, *Nano Lett.*, 2003, **3**, 403–407.
11 A. Star, T. R. Han, J. Christophe, P. Gabriel, K. Bradley and G. Gruner, *Nano Lett.*, 2003, **3**, 1421–1423.
12 M. Zhang, K. Gong, H. Zhang and L. Mao, *Biosens. Bioelectron.*, 2005, **20**, 1270–1276.
13 R. J. Chen, Y. Zhang, D. Wang and H. Dai, *J. Am. Chem. Soc.*, 2001, **123**, 3838–3839.
14 Y. Yan, M. Zhang, K. Gong, L. Su, Z. Guo and L. Mao, *Chem. Mater.*, 2005, **17**, 3457–3463.
15 G. Han, J. Yuan, G. Shi and F. Wei, *Thin Solid Films*, 2005, **474**, 64–69.
16 U. Yogeswaran, S. Thiagarajan and S. M. Chen, *Anal. Biochem.*, 2007, **365**, 122–131.
17 E. Frackowiak, V. Khomenko, K. Jurewicz, K. Lota and F. Béguin, *J. Power Sources*, 2006, **153**, 413–418.
18 N. Wahba, M. F. El Asmar and M. M. El Sadr, *Anal. Chem.*, 1959, **31**, 1870–1871.
19 I. M. Kolthoff and E. M. Carr, *Anal. Chem.*, 1953, **25**, 298–301.
20 S. M. Chen and S. H. Hsueh, *J. Electroanal. Chem.*, 2004, **566**, 291–303.
21 W. Guo, L. Xu, F. Li, B. Xu, Y. Yang, S. Liu and Z. Sun, *Electrochim. Acta*, 2010, **55**, 1523–1527.
22 H. W. Chu, R. Thangamuthu and S. M. Chen, *Electrochim. Acta*, 2008, **53**, 2862–2869.
23 H. Su, R. Yuan, Y. Chai, Y. Zhuo, C. Hong, Z. Liu and X. Yang, *Electrochim. Acta*, 2009, **54**, 4149–4154.
24 D. R. S. Jeykumari and S. S. Narayanan, *Biosens. Bioelectron.*, 2008, **23**, 1404–1411.
25 M. A. Thompson, *J. Am. Chem. Soc.*, 1995, **117**, 11341–11344.
26 G. M. Morris, D. S. Goodsell, R. S. Halliday, R. Huey, W. E. Hart, R. K. Belew and A. J. Olson, *J. Comput. Chem.*, 1998, **19**, 1639–1662.
27 J. Fuhrmann, A. Rurainski, H.-P. Lenhof and D. Neumann, *J. Comput. Chem.*, 2010, **31**, 1911–1918.
28 E. Meaurio, E. Zuza, N. López-Rodríguez and J. R. Sarasua, *J. Phys. Chem. B*, 2006, **110**, 5790–5800.
29 S. M. Chen and K.-C. Lin, *J. Electroanal. Chem.*, 2001, **511**, 101–114.
30 S. M. Chen and M.-I. Liu, *Electrochim. Acta*, 2006, **51**, 4744–4753.
31 J.-H. Song, D.-K. Choi and W.-K. Choi, *Nucl. Instrum. Methods Phys. Res., Sect. B*, 2002, **196**, 275–278.
32 M. Kajita, T. Kuwabara, D. Hasegawa and M. Yagi, *Green Chem.*, 2010, **12**, 2150–2152.
33 H. O. Finklea, D. A. Snider and J. Fedyk, *Langmuir*, 1993, **9**, 3660–3667.
34 A. Mohadesi and M. A. Taher, *Sens. Actuators, B*, 2007, **123**, 733–739.
35 C. P. Andrieux, O. Haas and J. M. SavGant, *J. Am. Chem. Soc.*, 1986, **108**, 8175–8182.
36 Y. Umasankar, A. P. Periasamy and S. M. Chen, *Talanta*, 2010, **80**, 1094–1101.
37 Y. T. Chang, K. C. Lin and S. M. Chen, *Electrochim. Acta*, 2005, **51**, 450–461.
38 S. M. Chen and C. M. Chan, *J. Electroanal. Chem.*, 2003, **543**, 161–173.
39 S. M. Chen and J. L. Lin, *J. Electroanal. Chem.*, 2004, **571**, 223–232.

